

# High Energy Dynamic Impact Testing of APC AS4D/PEKK-FC and TC1225 LMPAEK T700G Thermoplastic Composite Materials

J. Michael Pereira<sup>1</sup>, Sandi Miller<sup>2</sup>, Duane Revilock<sup>1</sup>, Charles Ruggeri<sup>1</sup>

*NASA Glenn Research Center, Cleveland, OH, 44135, U.S.A.*

Richard Martin<sup>3</sup>

*HX5, LLC, Cleveland, OH, 44135, U.S.A.*

**High energy dynamic impact tests were conducted on Solvay APC AS4D/PEKK-FC and Toray TC1225 LMPAEK T700G thermoplastic composite laminates. The primary objective was to provide data for evaluation of computational composite impact models. Empirical results indicate an approximately 50% increase in penetration threshold velocity and over 100% increase in penetration energy threshold for the TC1225 LMPAEK T700G composite compared to the APC AS4D/PEKK-FC composite. The velocity required to produce NDE-detectable delamination in the TC1225 LMPAEK T700G composite was roughly twice that for the APC AS4D/PEKK-FC composite. Comparison of the normalized energy absorption showed similar results for the APC AS4D/PEKK-FC system compared to a previously studied IM7/8552 composite material. The TC1225 LMPAEK T700G system absorbed approximately twice that of the other two systems when normalized by areal weight.**

## I. Introduction

Advances in physics-based, predictive models for simulating the high energy dynamic impact response of fiber-reinforced polymer composite materials and structures have led to the need for more extensive material property input data as well as experimental data for model evaluation and validation. Recently, new composite impact models have been proposed to address needs in the aerospace and automotive industries (B. Justusson, M. Molitor, et al. 2021, R. Goldberg, et al. 2016, Achstetter 2019, R. Goldberg, et al. 2018). Some of these new developments are motivated by the desire to create models that base their predictions, as much as possible, on coupon-level material properties, rather than relying on the adjustment of model parameters to produce a good correlation between the model predictions and structural level test results. An objective is to limit the number of structural level tests to those needed for model validation, rather than model correlation.

---

<sup>1</sup> Research Aerospace Engineer

<sup>2</sup> Chemical Engineer

<sup>3</sup> Senior Researcher

Several experimental efforts have been conducted to obtain the specific types of input properties required by these new models (Khaled, et al. 2018, B. Justusson, et al. 2020, Haluza, et al. 2020) and additional experimental programs have been conducted to provide model validation data (Justusson, Pang, et al. 2019).

The primary objective of this work was to conduct impact testing to provide data for evaluation of computational models applied to ballistic penetration problems with thermoplastic composite materials. Ballistic impact tests were conducted using a slight modification of the ASTM D8101 test standard (ASTM, 2018) on two different carbon fiber thermoplastic matrix composites, namely Solvay APC AS4D/PEKK-FC composite material and Toray TC1225 LMPAEK T700G composite material. Quantitative measurements of panel displacements during the impact event, damage, and velocity and energy penetration threshold were obtained.

## II. Methods

Instrumented ballistic impact tests were conducted on two thermoplastic quasi-isotropic laminated tape composite flat panels over an impact velocity range spanning that required to produce no detectable delamination using ultrasonic non-destructive evaluation (NDE), detectable delamination but no penetration, and full penetration of the panel by the projectile. In the tests the full field deformation and strain, the extent and type of damage to the panels, the onset of NDE-detectable delamination and the threshold penetration velocity and energy were measured.

### Materials

Test panels consisted of 32-ply flat quasi-isotropic laminated tape with a layup of  $[45/0/-45/90]_{4s}$  made up of two different thermoplastic matrix composite materials, Solvay APC AS4D/PEKK-FC and Toray TC1225 LMPAEK T700G. Nominal properties of the materials, listed in Table 1, were obtained from the manufacturers' specification sheets [Solvay, 2017, Toray Advanced Composites, 2020]. The panels were fabricated by the manufacturers in accordance with the standard manufacturing procedures and supplied to NASA. All the as-received panels were ultrasonically inspected prior to testing to ensure there was no pre-existing damage, and after testing to measure the impact damage.

The test panels received from Solvay were 12-inch square. Twenty-eight mounting holes were machined in the panels using a waterjet process. The panels received from Toray were nominally 12-inches x 16-inches and the holes were machined in the center portion of the panels without trimming to the standard 12-inch square geometry.

### Impact Testing

Impact testing was conducted in accordance with a modified version of the ASTM D8101 standard test method (ASTM 2018). The modification was to raise the mass of the projectile to 92 g from the standard 50 g projectile. This was done because the materials tested were slightly thicker than the panel thickness recommended in the test standard, and it was expected that the toughness of the materials could be higher than typical thermoset composite materials.

Table 1. Nominal composite properties

	Solvay APC AS4D/PEKK-FC	Toray TC1225 LMPAEK T700G
Resin Content (wt. %)	34	34
Cured Ply Thickness (mm)	0.14	0.14
Fiber Areal Weight (g/m <sup>2</sup> )	145	145
Ply Areal Weight (g/m <sup>2</sup> )	220 <sup>a</sup>	221 <sup>b</sup>

<sup>a</sup> Computed from resin content percent and fiber areal weight

<sup>b</sup> from specification sheet

The D8101 test method utilizes a flat test panel sandwiched between a circular front frame, with a 254-mm (10-inch) aperture, and a massive rear frame with 28 through-bolted shoulder bolts as shown in figure 1. A cup-shaped projectile with a radiused nose, shown in figure 2, is accelerated toward the specimen in free flight and impacts the specimen at the center in the normal direction. Typically, the projectile either fully penetrates the specimen or rebounds. In relatively few cases it embeds itself in the specimen. For the tests discussed here, high speed cameras and photogrammetry were used to measure the projectile impact velocity and orientation and the rebound or exit velocity. High speed 3D digital image correlation (DIC) was used to measure full-field deformation and calculate strains on the back side of the panels.

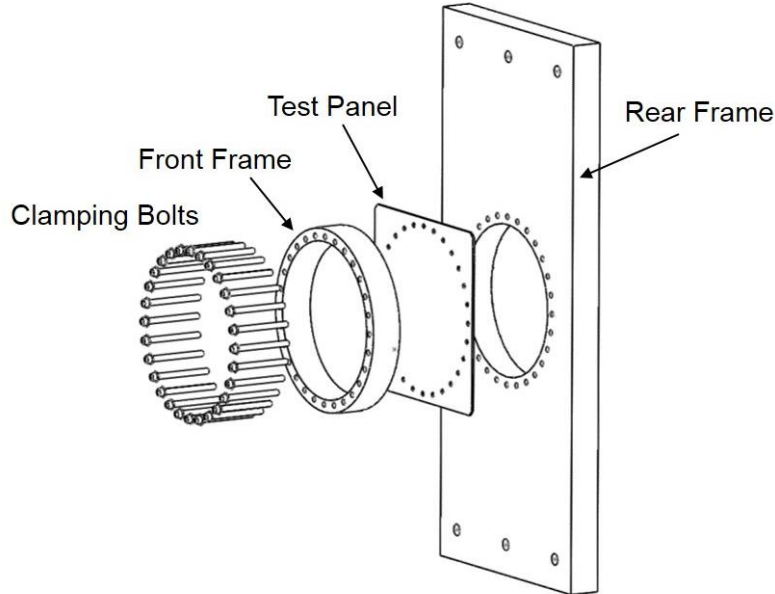


Figure 1. Overall view of the specimen and test fixture.

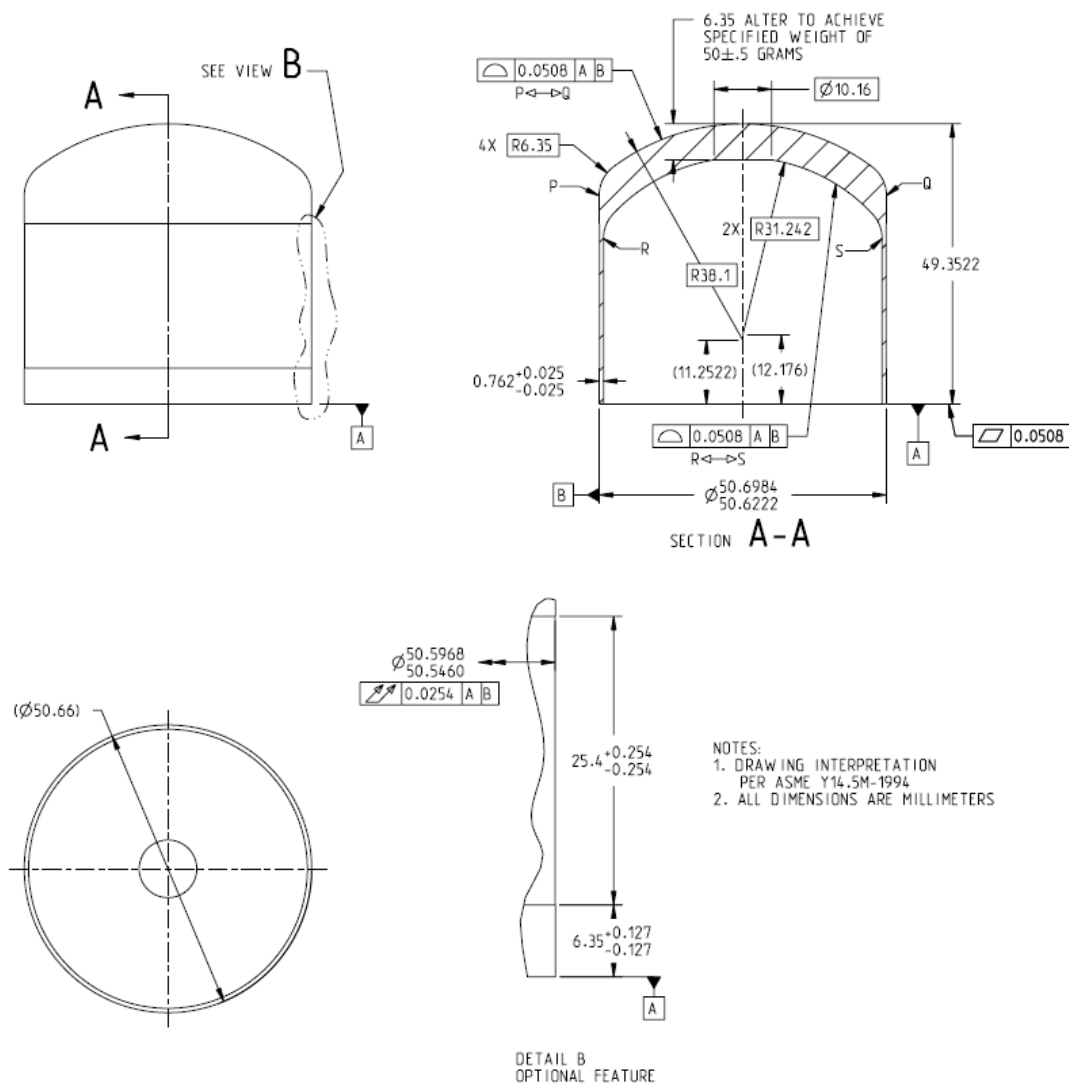


Figure 2. Standard ASTM D8101 Projectile. Projectile for this study had a thicker nose to raise the mass to 92 g.

## Impact Gun

The projectiles were accelerated with a single stage gas gun connected to a vacuum chamber, shown in figure 3, using compressed nitrogen as the propellant. The gun barrel had a length of 7.1-m (23.3-feet) and a bore of 50.8 mm (2.0 inches). The projectile fit freely in the bore of the gun barrel and was accelerated without the use of a sabot. The pressure vessel was made up of sections as shown in figure 4, with a total volume of 31-L (1900-in<sup>3</sup>). The gun barrel protruded into the vacuum chamber which held the fixture for the specimens. For this series of tests, the test chamber was maintained at normal atmospheric pressure.



Figure 3. Gas gun connected to the vacuum chamber.



Figure 4. Pressure Vessel.

## Instrumentation

High speed cameras were used to obtain photogrammetric data and digital image correlation data. Two calibrated pairs of cameras viewed the area in front of the specimen and the area behind the specimen to measure the projectile impact velocity and orientation and the rebound or exit velocity. The cameras were located above the test chamber and viewed the area through a polycarbonate porthole. A pair of cameras viewed the rear side of the panels to obtain digital image correlation (DIC) displacement results. In addition, there was a camera viewing the projectile from the side to provide a redundant measurement of impact velocity. A camera view from the front provided an overall view of the impact area.

The GOM ARAMIS DIC system (Trilion Quality Systems, King of Prussia, PA) was used for measuring the panel displacements. Displacement results measured by DIC are in a coordinate system centered on the rear of the test panel with the x-axis to the right, when facing the back side of the panel, the y-axis upward and the z-axis in the direction of the axis of the gun barrel. This coordinate system is separate and different than the one used for measuring projectile orientation, discussed in the following paragraphs.

The orientation of the projectile was measured by establishing a fixed lab coordinate system as well as a local coordinate system on the projectile. In the fixed coordinate system, the X-axis pointed in the direction of the gun barrel, the Y-direction was horizontally to the left when viewing the specimen from the gun barrel and the Z-direction was vertically up. The directions of these vectors were defined from fixed points in the test chamber that were viewable by both cameras.

To measure the orientation of the projectile in flight, a precisely located set of circular dots was painted on the projectile with the use of a cylindrical template which allowed repeatability between all projectiles. The local coordinate system of the projectile was defined by this dot pattern and the projectile was placed in the gun barrel in such a way that the local coordinate system of the projectile was initially parallel to the lab coordinate system. A vector defining the axis of the cylinder defined by the dot pattern was established. The orientation of the projectile was defined by the projection of this axis on the fixed lab XZ and XY planes. The angles from the X-axis to these projections were termed pitch and yaw, respectively. The roll angle (rotation about the axis of the projectile) was not considered.

## Non-destructive Evaluation (NDE)

Ultrasonic C-scans were used to evaluate the panels before and after impact testing. The immersion scans were done using a single 5 MHz focused transducer in the pulse-echo configuration with 1mm scan and step increments, with the impacted side of the panel facing the transducer. The scans showed the amplitude of the back-wall echo. The C-scans were taken from the front (impact side) of the panel. When comparing these images to the DIC data taken on the back side of the panel it should be noted that the positive x-direction of the DIC data corresponds to the leftward direction on the ultrasound images.

## III. Results

Thirteen tests were conducted on the Toray material and twelve tests on the Solvay material to establish the penetration velocity threshold, displacement, and damage measurements. Pre- and post-test ultrasound C-scan results and DIC results are shown in the Appendix. DIC was possible in cases where debris from the panel impact did not obscure the paint pattern.

### Toray TC1225 LMPAEK T700G Material

Pre-test ultrasonic c-scan results for the Toray material indicated that all panels were good quality and well consolidated, with no areas of delamination, and the machining process introduced no delamination in the region of the holes.

Results from the impact tests on the Toray TC1225 LMPAEEK T700G test panels are shown in table 2. In the table the exit/rebound velocity is positive if the projectile penetrated the panel and negative if it rebounded.

Table 2. Impact Test Results for Toray TC1225 LMPAEEK T700G Material. Negative value for exit/rebound velocity indicates a rebound.

Test Number	Projectile Mass (g)	Impact Velocity (m/sec)	Exit/Reb. Velocity (m/sec)	Impact Energy (J)	Projectile Orientation (deg)		Penetration	UT Detectable Delamination
					Pitch	Yaw		
LVG1399	92.37	157.0	-71.4	1133.4	1.08	0.75	No	Yes
LVG1400	92.27	216.7	164.1	2160.4	1.787	0.807	Yes	Yes
LVG1401	92.26	171.0	Not avail.	1345.5	0.978	1.584	Yes	Yes
LVG1402	92.35	147.5	-69.9	1001.1	0.328	0.779	No	Yes
LVG1403	92.21	158.2	25.8	1151.6	1.132	1.253	Yes	Yes
LVG1404	92.22	151.7	-72.1	1058.6	1.387	0.401	No	Yes
LVG1405	92.32	154.2	-69.6	1094.2	0.482	2.485	No	Yes
LVG1406	92.27	73.8	-42.9	250.3	1.413	1.488	No	Yes
LVG1407	92.23	39.8	-30.6	72.8	1.818	1.07	No	No
LVG1408	92.11	49.0	-33.3	110.3	5.94	7.69	No	Yes
LVG1409	92.23	38.0	-28.8	66.5	0.993	0.354	No	No
LVG1410	92.18	39.5	-28.7	71.6	2.807	3.884	No	No
LVG1413	92.03	43.8	Not avail.	88.1	Not available		No	Yes

In general, the pitch and yaw angles were less than 2°, but in one of the lower velocity tests the projectile pitched down almost 3° and yawed almost 4°. At such low impact velocities, the effect of gravity on the location of impact becomes significant and resulted in the projectile impacting the panel below the center. It should be noted that measurements of the rebound velocity are somewhat approximate because the projectile was typically tumbling, and the center of mass could not be precisely identified. In addition, after impact propellant gas was typically still exiting the gun barrel, which could affect the velocity.

Figure 5 shows the impact results with the impact velocity on the abscissa and the penetration value on the ordinate, the values 0 and 1 corresponding to no-penetration and penetration respectively.

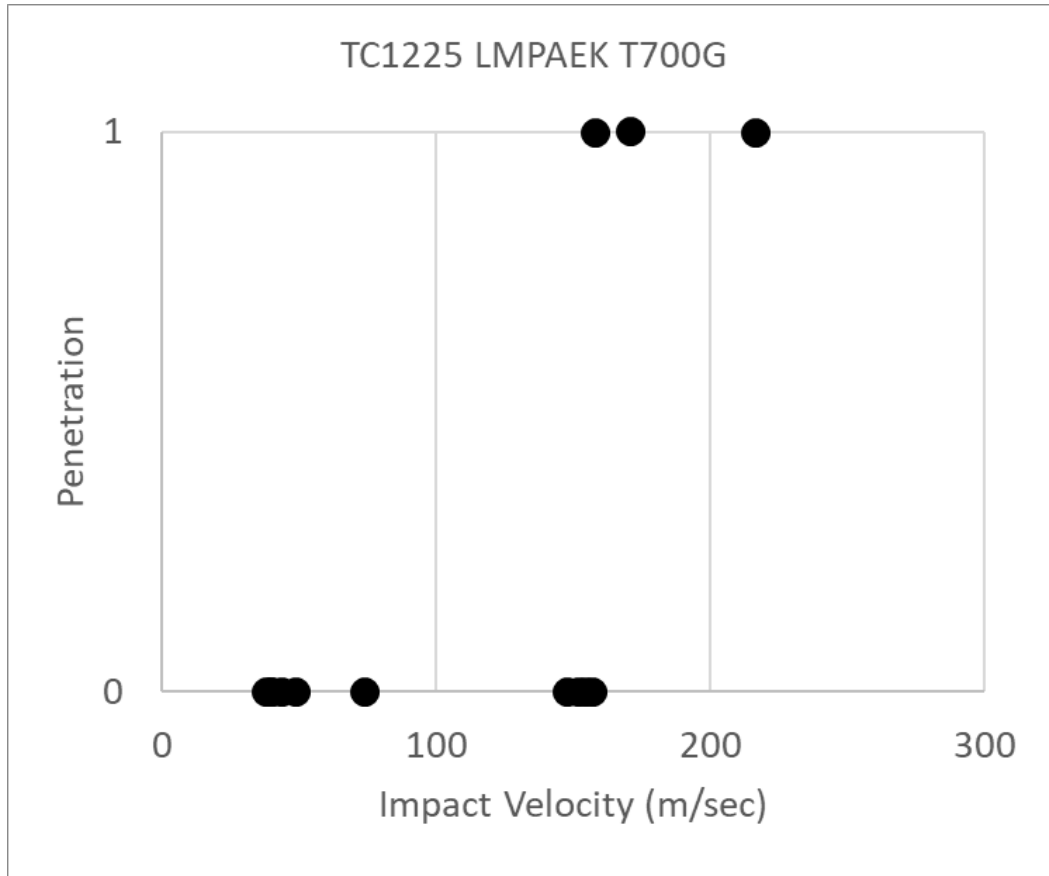


Figure 5. Penetration results for TC1225 LMPAEK T700G Panels.

For this material the onset of ultrasonically detectable delamination occurred between impact velocities of 39.5 and 43.8 m/sec.

The test with the highest velocity that did not penetrate was test LVG1399, with an impact velocity of 157.0 m/sec. The post-test scan of this test (figure 6) shows extensive delamination, spreading to most of the perimeter of the unclamped portion of the panel. Similar results are seen in the post-test scan of test LVG1403 (figure 7), which had the lowest penetrating impact velocity. At the highest impact velocity there was significantly less delamination as can be seen in figure 8.

Displacements measured during the impact and permanent displacement after the impact, measured by DIC, are available by contacting the authors. In some cases where penetration occurred it was not possible to obtain DIC data due to masking of the image from debris.

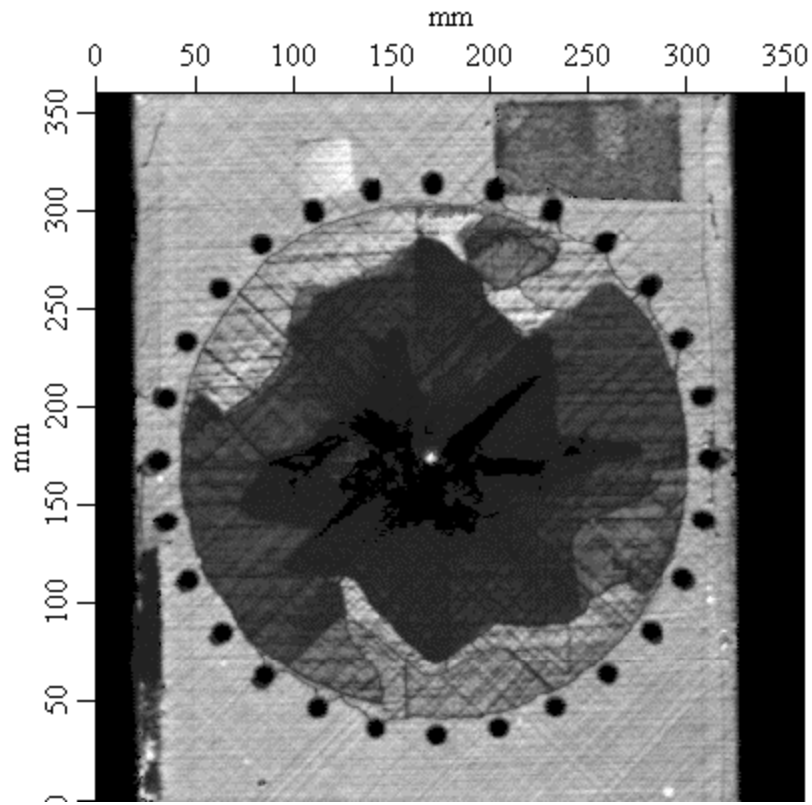


Figure 6. Post-test ultrasound scan of test LVG1399, the test with the highest non-penetrating impact velocity

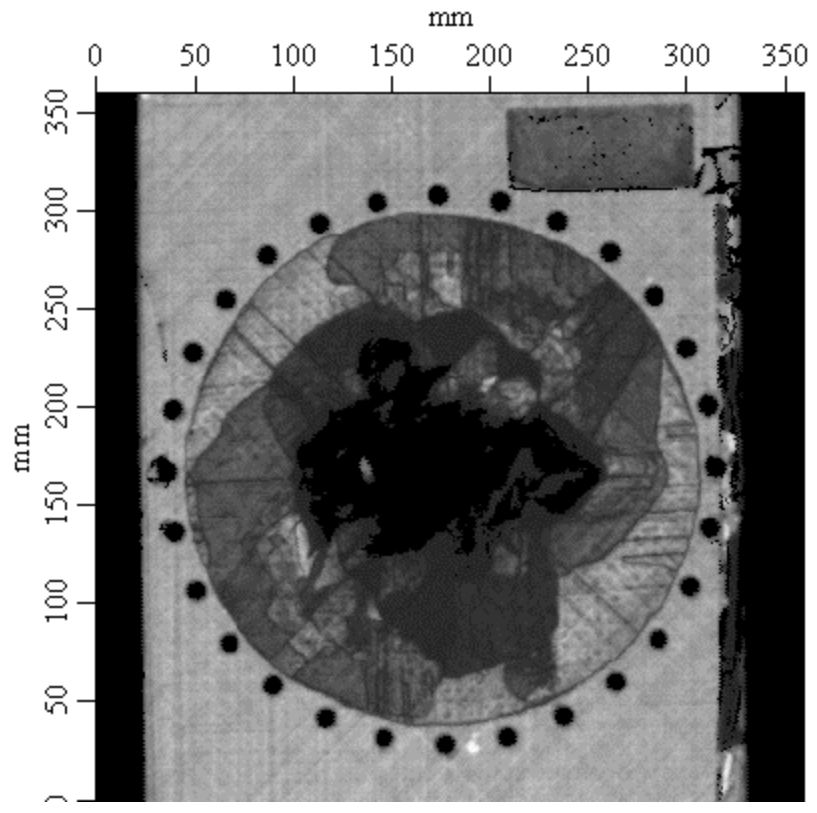


Figure 7. Post-test ultrasound scan of test LVG1403, the test with the lowest penetrating impact velocity

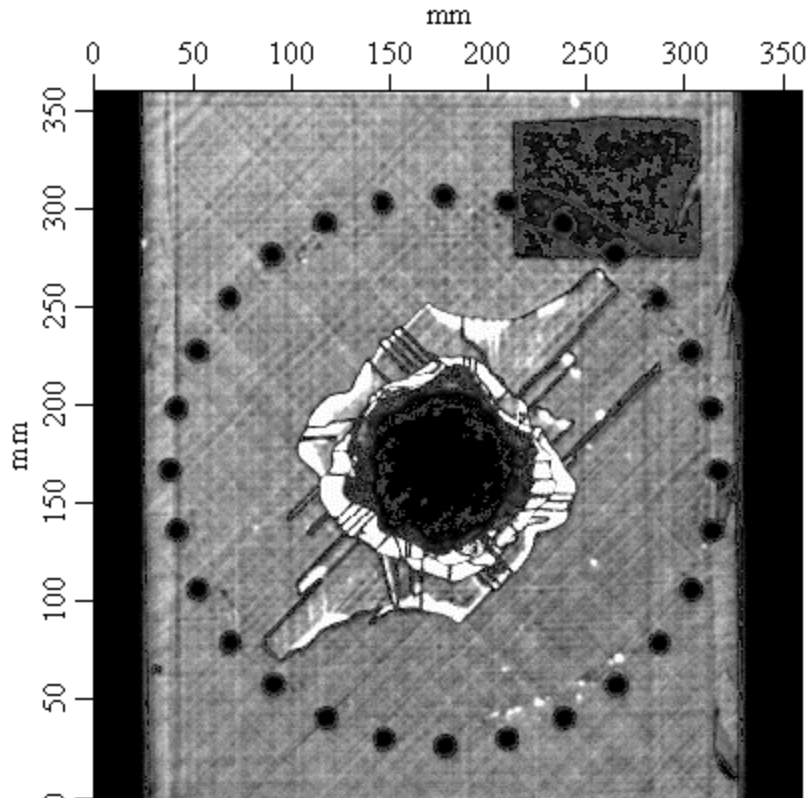


Figure 8. Post-test ultrasound scan of test LVG1400, the highest velocity test

### 3.2 Solvay APC AS4D/PEKK-FC Material

As with the Toray panels, pre-test ultrasonic c-scan results for the Solvay material indicated that all panels were good quality and well consolidated, with no areas of delamination, and the machining process introduced no delamination in the region of the holes.

Results from the impact tests on the Solvay APC AS4D/PEKK-FC test panels are shown in table 3. In the table the exit/rebound velocity is positive if the projectile penetrated the panel and negative if it rebounded. The pitch and yaw angles at impact are shown as well. In some cases, angles were higher than desired, especially at very low impact velocities where the orientation and velocity are more difficult to control with the apparatus used.

Table 3. Impact Test Results for Solvay APC AS4D/PEKK-FC Material. Negative value for exit/rebound velocity indicates a rebound.

Test Number	Projectile Mass (g)	Impact Velocity (m/sec)	Exit/Reb. Velocity (m/sec)	Impact Energy (J)	Projectile Orientation (deg)		Penetration	UT Detectable Damage
					Pitch	Yaw		
LVG1414	92.55	151.8	Not avail.	1066.3	0.823	0.511	Yes	Yes
LVG1415	92.4	115.5	64.5	616.3	0.258	0.908	Yes	Yes
LVG1416	92.33	98.8	-19.5	450.6	6.963	7.09	No	Yes
LVG1417	92.33	107.9	23.4	537.5	5.523	6.471	Yes	Yes
LVG1418	92.31	102.1	-38.7	481.1	1.142	1.17	No	Yes
LVG1419	92.32	105.8	Not avail.	516.7	Not available		No	Yes
LVG1420	92.41	30.2	-29.3	42.1	14.76	12.135	No	Yes
LVG1421	92.32	36	-30.1	59.8	21.04	9.55	No	Yes
LVG1423	92.18	27.1	-20.4	33.8	8.37	4.61	No	Yes
LVG1425	92.57	11.4	-8.5	6.0	6.83	7.49	No	No
LVG1426	92.56	8.8	-6.1	3.6	3.1	7.96	No	No
LVG1427	92.17	15.3	Not avail.	10.8	15.2	2	No	No

Figure 9 shows the impact results with the impact kinetic energy on the abscissa, with the same scale as figure 5, and the penetration value on the ordinate. The values 0 and 1 on the ordinate correspond to no-penetration and penetration respectively. For this material the onset of NDE-detectable delamination occurred between impact velocities of 14.5 and 27.1 m/sec.

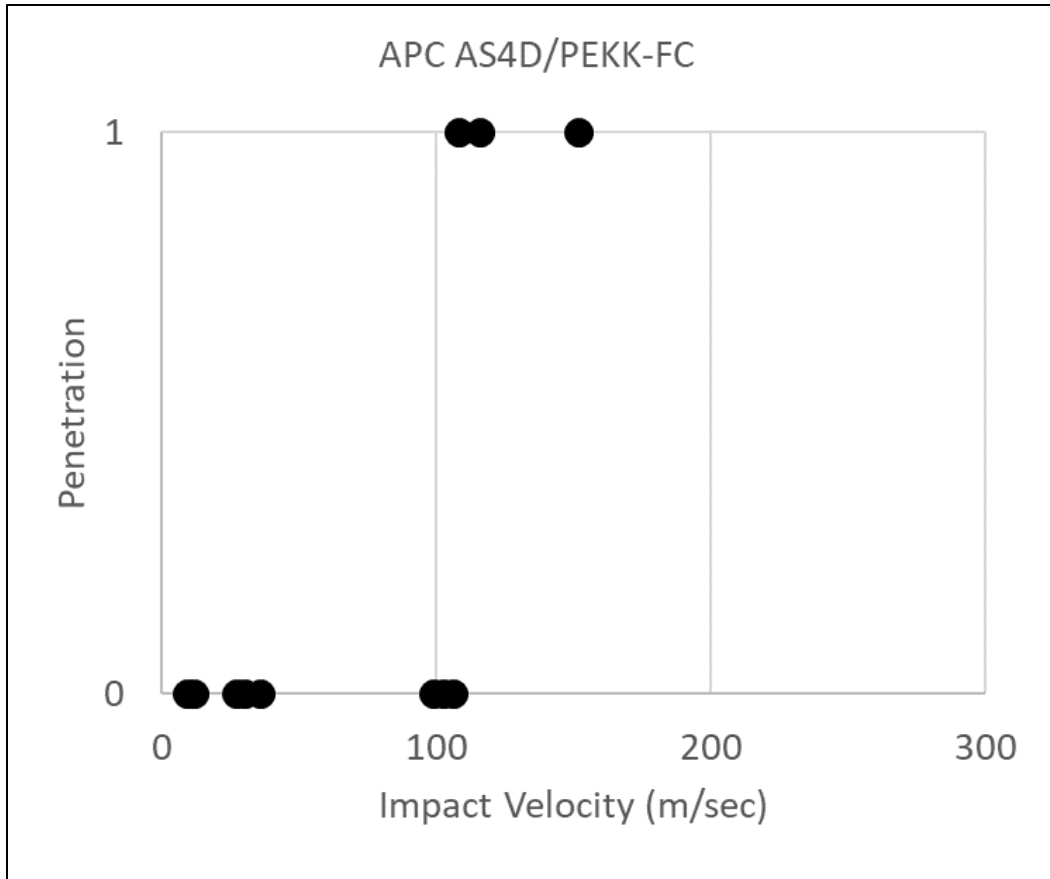


Figure 9. Penetration results for APC AS4D/PEKK-FC Panels.

The test with the highest velocity that did not penetrate was test LVG1419, with an impact velocity of 105.8 m/sec. The post-test scan of this test (figure 10) shows full delamination over the unclamped area of the specimen. There was slightly less delamination in test LVG1417 (figure 11), which had the lowest penetrating impact velocity. At the highest impact velocity there was significantly less delamination as can be seen in figure 12.

Displacements measured during the impact and permanent displacement after the impact, measured by DIC, are available from the authors. In some cases where penetration occurred it was not possible to obtain DIC data due to masking of the image from debris.

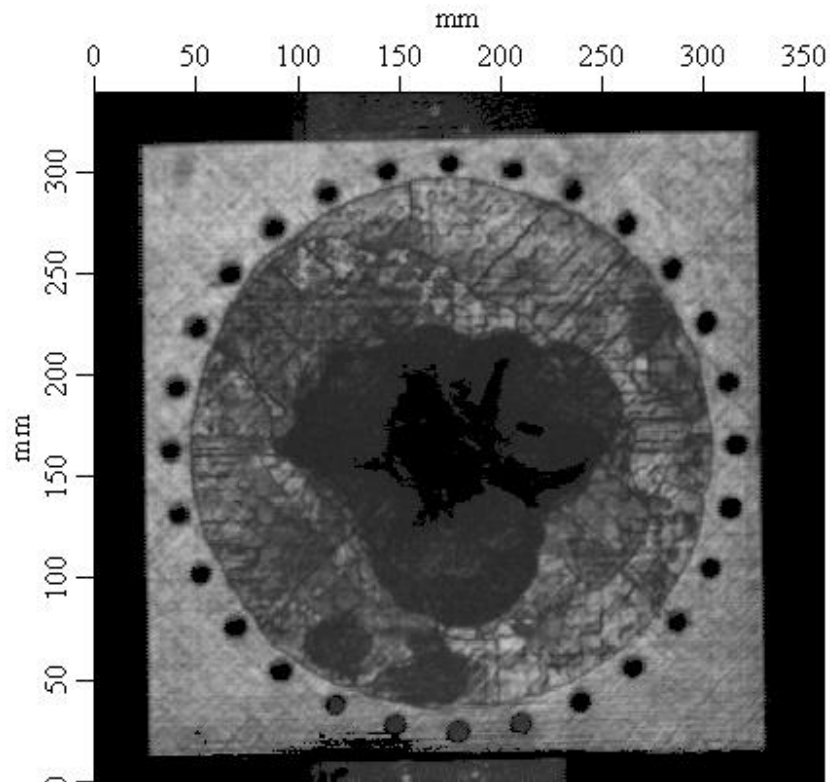


Figure 10. Post-test ultrasound scan of test LVG1419, the test with the highest non-penetrating impact velocity

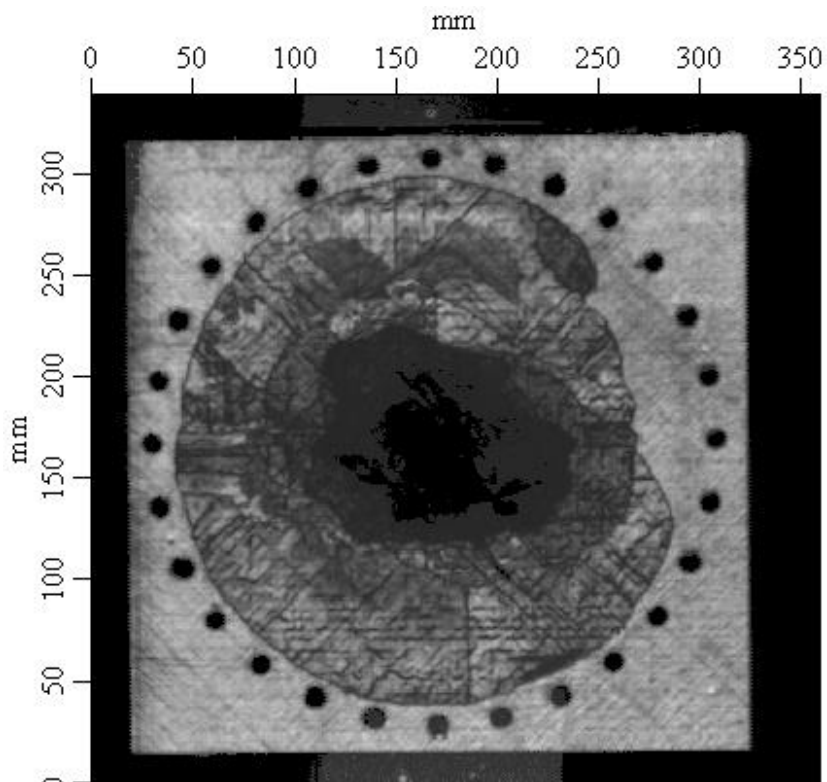


Figure 11. Post-test ultrasound scan of test LVG1417, the test with the lowest penetrating impact velocity

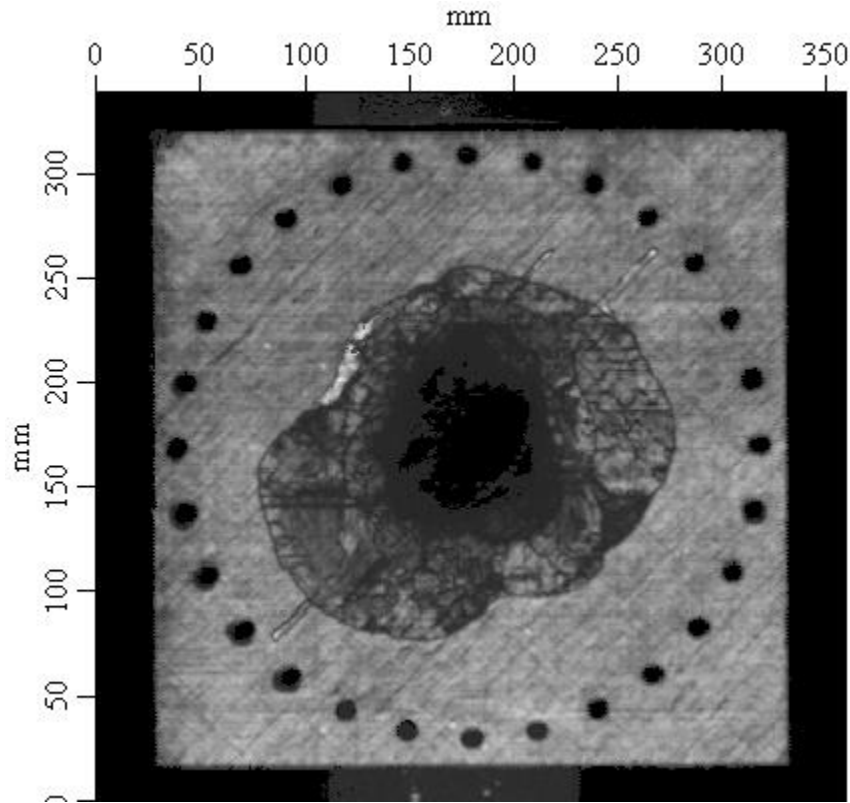


Figure 12. Post-test ultrasound scan of test LVG1414, the highest velocity test

### Comparison of Impact Results

A comparison of the summary impact results for the two materials tested in this study is shown in figure 13. For cases such as this where there is no overlap between the velocities of the tests in which penetration occurred and those where no penetration occurred, the penetration velocity threshold is calculated from the average of the highest non-penetration velocity and the lowest penetration velocity. For the TC1225 LMPAEK T700G material the penetration velocity threshold was 157.6 m/sec, yielding a penetration energy threshold of 1143 J. For the APC AS4D/PEKK-FC material the penetration velocity threshold was 106.8 m/sec, yielding a penetration energy threshold of 524.7 J. The impact velocities resulting in the onset of NDE-detectable delamination for the two materials are shown graphically in figure 14.

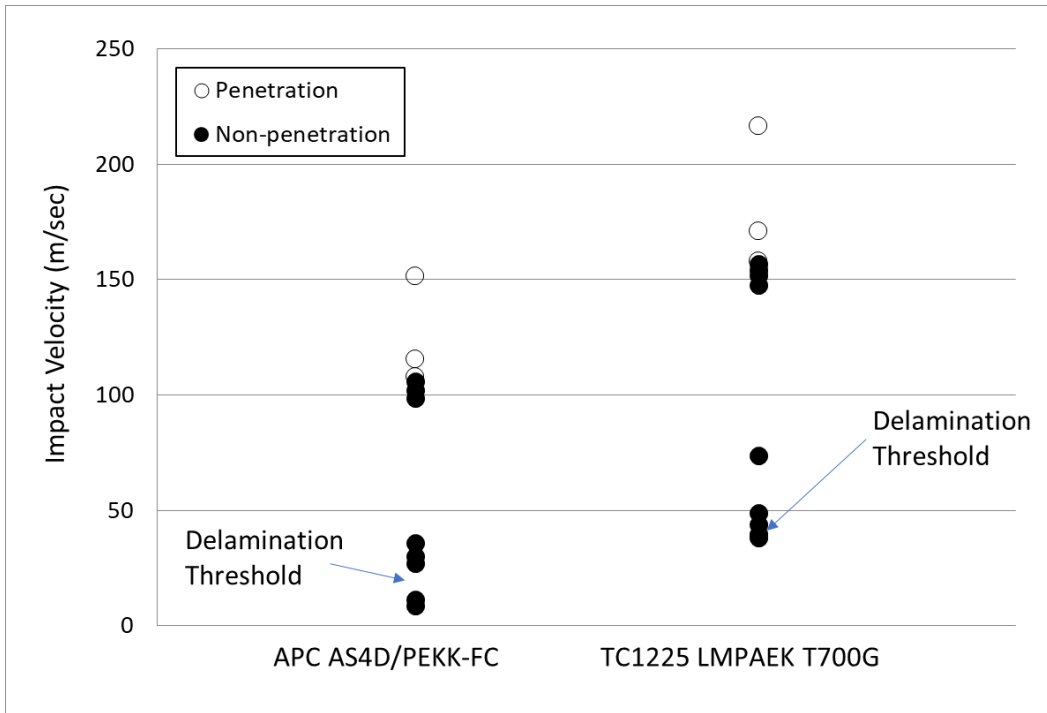


Figure 13. Impact test results for the APC AS4D/PEKK-FC and TC1225 LMPAEK T700G materials showing the relative velocity penetration thresholds and onset of NDE-detectable delamination.

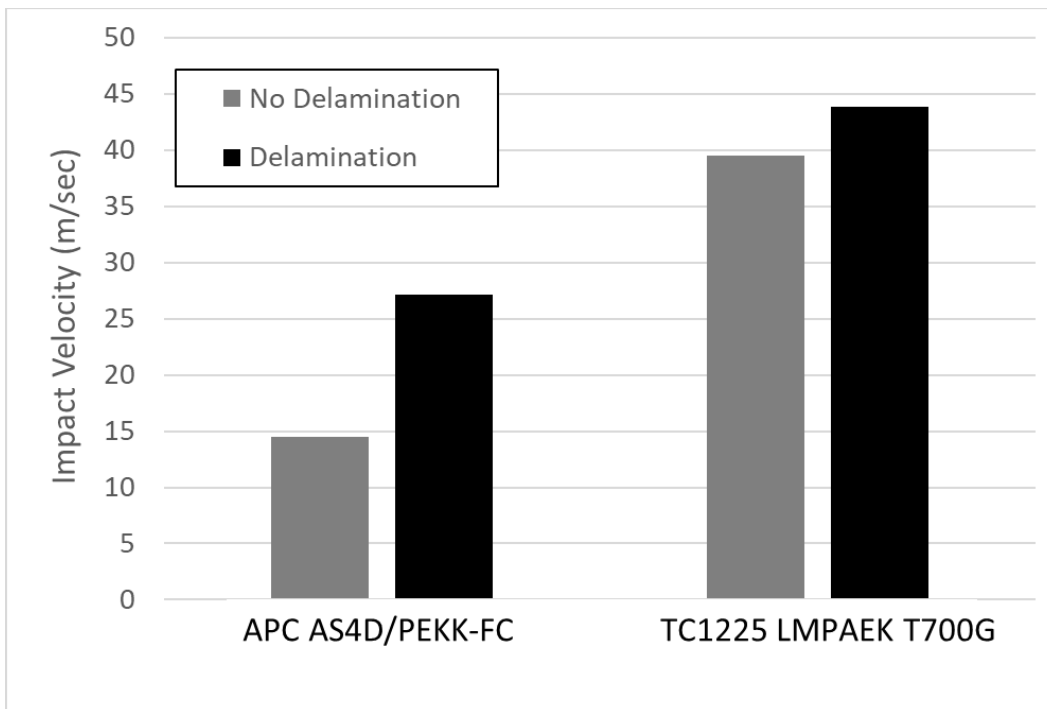


Figure 14. Impact velocities for tests near the onset of NDE-detectable delamination for the APC AS4D/PEKK-FC and TC1225 LMPAEK T700G materials

It is useful to compare the penetration threshold results of the two material systems tested in this study with available data from a thermoset composite material. In a previous study similar testing was conducted on quasi-isotropic laminated tape composite material consisting of Hexcel IM7 fibers and 8552 thermoset resin [NASA Advanced Composites Project, Midyear Review, Oct. 2017]. This material was a 40-ply laminate with a  $[45/90/-45/0]_{5S}$  layup. While the thickness and number of plies are different, the layup is similar, and the test fixture and projectile are the same. It is possible to compare penetration threshold results normalized by panel areal mass.

Figure 15 shows the normalized penetration energy threshold for the two thermoplastic systems used for this study and the previously tested thermoset composite. The plotted value is the penetration energy threshold normalized by the total areal weight of the composite (number of plies x ply areal weight). For the thermoplastic systems the ply areal weight is taken from table 1. The areal weight for the IM7/8552 thermoset material is calculated from values given by Ng and Tomblin (2013). This value of  $292 \text{ g/m}^2$  is calculated using values for fiber areal weight of  $190 \text{ g/m}^2$  and a resin content of 35%.

These results indicate similar energy absorption by weight of the IM7/8552 material and the APC AS4D/PEKK-FC material and approximately double the normalized energy absorption for the TC1225 LMPAEK T700G system.

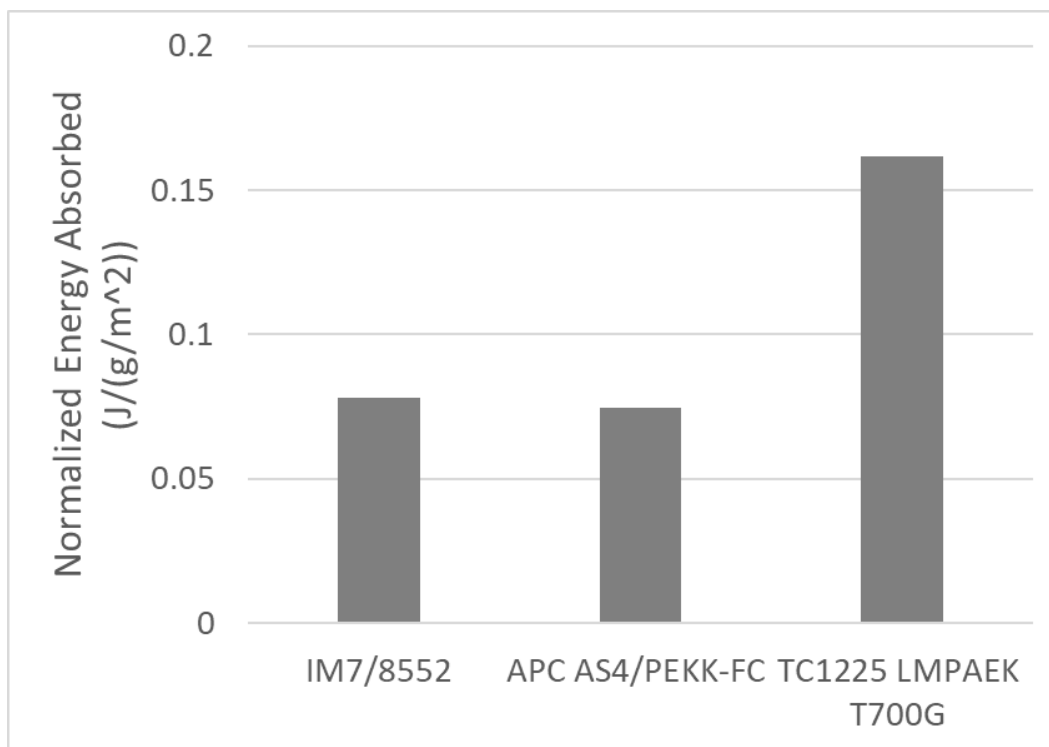


Figure 15. Penetration energy threshold normalized by composite areal weight

## IV. Summary and Conclusions

Data are presented here for two thermoplastic composite laminates from impact tests conducted using the ASTM D8101 test standard. The primary objective is to provide data for evaluation of computational composite impact models. Detailed quantitative tabular data are available from the authors.

Empirical results indicate an approximately 50% increase in penetration threshold velocity and over 100% increase in penetration energy threshold for the TC1225 LMPAEK T700G composite compared to the APC AS4D/PEKK-FC composite. The velocity required for NDE-detectable delamination in the TC1225 LMPAEK T700G composite was roughly twice that for the APC AS4D/PEKK-FC composite.

Comparison of the normalized energy absorption showed similar results for the APC AS4D/PEKK-FC system compared to a previously studied IM7/8552 composite material. The TC1225 LMPAEK T700G system absorbed approximately twice that of the other two systems.

## V. References

Achstetter, T. 2019. "Development of a composite material shell-element model for impact applications." Ph.D. Dissertation. George Mason University.

ANSYS/LST. n.d. Livermore Software Technology. Accessed February 24, 2021.  
<https://www.lstc.com/download/manuals>.

ASTM. 2018. "D8101/D8101M, Standard test method for measuring the penetration resistance of composite materials to impact by a blunt projectile." West Conshohocken, PA: ASTM International. doi:10.1520/D8101\_D8101M-18.

Goldberg, R.K., K.S. Carney, P. DuBois, C. Hoffarth, J. Harrington, S. Rajan, and G. Blankenhorn. 2016. "Development of an orthotropic elasto-plastic generalized composite material model suitable for impact problems." *Journal of Aerospace Engineering* 29 (4).

Goldberg, R.K., K.S. Carney, P. DuBois, C. Hoffarth, L. Shyamsunder, S. Rajan, and G. Blankenhorn. 2018. "Implementation of a tabulated failure model into a generalized composite material model." *Journal of Composite Materials* 52 (25): 3445-3460.

Haluza, R.T., K. Koudela, C. Bakis, D.O. Adams, M.A. Perl, and M. Pereira. 2020. "Out-of-plane shear properties of IM7/8552 carbon/epoxy by v-notch shear testing." *AIAA Scitech 2020 Forum*. 1212.

Justusson, B., J. Pang, M. Molitor, M. Rassaian, and R. Rosman. 2019. "An overview of the NASA Advanced Composites Consortium High Energy Dynamic Impact Phase II Technical Path." *AIAA 2019 Scitech*. San Diego.

Justusson, B., M. Molitor, J. Schaefer, and S. Liguore. 2021. "The use of LS-DYNA MAT299 for Accurate Prediction of Impact Damage in Composite Structures." *AIAA SciTech 2021 Forum*. Nashville: AIAA.

Justusson, B.P., M.J. Molitor, J.S. Iqbal, M. Rassaian, T.M. Ricks, and R.K. Goldberg. 2020. Overview of coupon testing of an IM7/8552 composite required to characterize high-energy impact dynamic material models. TM 2020-220498, NASA.

Khaled, B., L. Shyamsunder, N. Schmidt, C. Hoffarth, and S. Rajan. 2018. Development of a tabulated material model for composite material failure, MAT213. Part 2: Experimental tests to characterize the behavior and properties of T800-F3900 Toray Composite. DOT/FAA/TC-19/51, Nov., Washington, D.C.: Federal Aviation Administration.

Ng, Y. and Tomblin, J. 2013. NCAMP Material Specification Hexcel 8552 IM7 Unidirectional Tape. NMS 128/2, Revision B, Wichita: National Institute for Aviation Research.

Photron, Inc. n.d. Photron. Accessed February 24, 2021. <https://photron.com/>.

Solvay. 2017. Technical Data Sheet APC (PEKK-FC) PEKK-FC THERMOPLASTIC POLYMER PREPREG. October 11. Accessed April 16, 2022. [https://catalogservice.solvay.com/downloadDocument?fileId=MDkwMTY2OWM4MDU0YjY0OQ==&fileName=APC-PEKK-FC\\_CM\\_EN.pdf&base=FAST](https://catalogservice.solvay.com/downloadDocument?fileId=MDkwMTY2OWM4MDU0YjY0OQ==&fileName=APC-PEKK-FC_CM_EN.pdf&base=FAST).

Toray Advanced Composites. 2020. Toray Cetex(R) TC1225. April 22. Accessed April 16, 2022. [https://www.toraytac.com/media/3bd72fac-0406-48e4-bfc4-2ffd2398ac0c/zipxIA/TAC/Documents/Data\\_sheets/Thermoplastic/UD%20tapes,%20prepregs%20and%20laminates/Toray-Cetex-TC1225\\_PAEK\\_PDS.pdf](https://www.toraytac.com/media/3bd72fac-0406-48e4-bfc4-2ffd2398ac0c/zipxIA/TAC/Documents/Data_sheets/Thermoplastic/UD%20tapes,%20prepregs%20and%20laminates/Toray-Cetex-TC1225_PAEK_PDS.pdf).

Vision Research, Inc. n.d. Phantom Ametek. Accessed February 24, 2021. <http://www.phantomhighspeed.com>